NANO LETTERS

2008
Vol. 8, No. 8
2161-2165

Tip-Modulation Scanned Gate Microscopy

Neil R. Wilson*,† and David H. Cobden‡

Department of Physics, University of Warwick, Coventry, CV4 7AL, U.K., and
Department of Physics, University of Washington, Seattle, Washington 98195-1560

Received February 19, 2008; Revised Manuscript Received May 27, 2008

ABSTRACT

We introduce a technique that improves the sensitivity and resolution and eliminates the nonlocal background of scanned gate microscopy (SGM). In conventional SGM, a voltage bias is applied to the atomic force microscope tip and the sample conductance is measured as the tip is scanned. In the new technique, which we call tip-modulation SGM (tmSGM), the biased tip is oscillated and the induced oscillation of the sample conductance is measured. Applied to single-walled carbon nanotube network devices, tmSGM gives sharp, low-noise and background-free images.

Atomic force microscopy (AFM) can be used in a number of ways to study the electrical properties of nanoscale structures by applying a voltage, V_{tip}, to the scanning tip. The most common techniques of this kind are electrostatic force microscopy (EFM), conducting AFM, and scanned capacitance microscopy, which can be used to infer for example the local potential, conductivity, and dopant concentration (for a review see ref 1). Less widely known is scanned gate microscopy (SGM),[2–13] in which the current through the device is measured while scanning the AFM tip above the sample surface. The tip bias alters the electrostatic potential and free charge density at the surface beneath, so the tip acts as a small scanning local gate electrode. If the sample is nonuniform, the associated change in conductance depends on the tip position and an image of tip bias sensitivity ("local transconductance") versus position can be constructed, giving information about such things as current distribution, location of potential barriers, and free charge density in the sample.

One reason SGM is relatively rarely used is that it is limited by the slow (reciprocal) decay of capacitance with distance, leading to a large nonlocal background signal from the capacitance to the tip cone and the cantilever. A second reason is that for many systems of interest, such as thin films, the total conductance is only weakly dependent on the modification of a small region by the tip, and so the signal is too small to be practical. This is not a problem for one-dimensional (1D) structures such as carbon nanotubes and nanowires where the sensitivity to local gating can be large because a small part of the nanotube can limit the total conductance. For this reason SGM has been used extensively on nanotube devices, where it has revealed the disordered background potential in semiconducting nanotubes,[2,3] resistance contributions due to defects[4,5] and Schottky barriers at the contacts,[6] resonant energy dependence of scattering by defects,[7] and single electron charging effects.[8] SGM has also been used successfully on nanowire devices[9] and on low temperature systems such as quantum point contacts[10–12] and microconstrictions[13] in two-dimensional (2D) electron gases where sensitivity to a local perturbation is enhanced.

Here we employ a simple and practical extension of SGM, which we term tip-modulation SGM (tmSGM), that results in better sensitivity and resolution and in rejection of nonlocal contributions. As usual, a dc voltage is applied to the tip, but now the tip is oscillated, and the amplitude of the induced conductance oscillations is measured using a lock-in amplifier. The resulting signal is proportional to the derivative of the tip−sample capacitance with respect to tip height, which is a more local quantity than the capacitance, analogous to the situation in force-sensitive EFM.[14,15] This offers the possibility of applying scanned gate techniques to a wider range of samples than before. Applied to 2D single-walled carbon nanotube network devices, for example, we show that tmSGM gives sharp, low-noise and background-free images. In contrast to the SGM image, features in the tmSGM image are sufficiently resolved to be connected unambiguously with specific structures in the nanotube networks.

In conventional SGM, illustrated in Figure 1a, a bias voltage V_{sd} is applied between source and drain contacts, and the resulting current is converted to a voltage (we use an Ithaco 1211 current preamplifier) which is recorded by

* Corresponding author. E-mail: Neil.Wilson@warwick.ac.uk.
† University of Warwick.
‡ University of Washington.

10.1021/nl080488i CCC: $40.75
Published on Web 06/27/2008

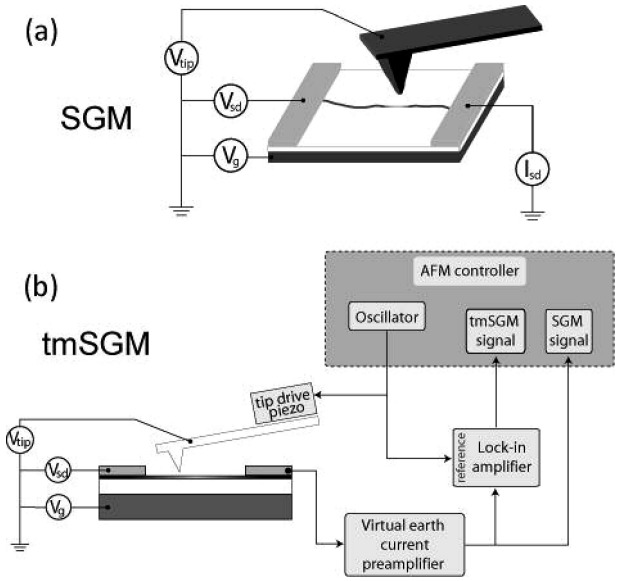

Figure 1. Schematics of the setup for (a) scanned gate microscopy (SGM) and (b) simultaneous SGM and tip-modulation scanned gate microscopy (tmSGM).

the AFM controller. SGM images are taken in "lift mode": the tip scans each line twice, first in tapping mode with zero tip bias to determine the topography, and then again at a set distance l_h above the surface, with V_{tip} applied. In tmSGM, illustrated in Figure 1b, the cantilever is driven at its resonant frequency during the lift mode trace, and the preamplifier output is sent to a lock-in amplifier using the cantilever drive signal as its reference. The output of the lock-in, representing the amplitude of the current variation induced by the tip motion, is recorded by the AFM controller. SGM and tmSGM images can be acquired simultaneously by recording both the dc component of the preamplifier output and the lock-in output. We employed the technique successfully on two different AFM systems: a Veeco Multimode AFM with Nanoscope IIIa controller and Extender Module, and a Veeco Dimension 3100 AFM with Nanoscope IV controller. On both instruments we used uncoated degenerately doped Si tips with resonance frequencies <100 kHz, and with typical oscillation amplitudes of order 30 nm (root-mean-square).

To investigate the capability of tmSGM, we studied devices containing single-walled nanotubes, which are not only of intrinsic interest but are also useful for characterizing the spatial resolution and sensitivity of electrical scanned probe techniques due to their nanometer-scale diameters.[16,17] The nanotubes were grown by chemical vapor deposition on an oxidized silicon substrate and contacted by evaporated Au/Cr leads patterned by photolithography and lift-off. Figure 2a is a topographic image of a nanotube device which exhibits p-type semiconducting behavior. Figure 2 panels b and c are the simultaneously acquired SGM and tmSGM images. In both, one can see a series of blotches along the path of the nanotube, representing regions where the positive tip bias of +2.5 V decreases the conductance. The blotches might for instance be associated with positively charged defects on the substrate under the nanotube which cause a reduced hole density in the nanotube that is more quickly depleted.[5]

Figure 2d−f shows similar images of another single nanotube device. Figure 3 shows line profiles corresponding to the dashed lines in the SGM and tmSGM images. The tmSGM noise level is much lower, and the line width of the nanotube response is about half that in the SGM image. As a result, extra features can be resolved. The SGM response has a nonlocal contribution, visible in its slow (~micron-scale) decay back to steady state, which is not evident in the tmSGM signal. The better signal-to-noise ratio is a result of the lock-in detection scheme, which has in fact been employed for SGM before.[5] However, the improved resolution observed here and the absence of nonlocal background need more explanation.

To understand them, consider first the SGM image of a single sensitive point on a sample, such as a defect in an otherwise clean nanotube. The regular SGM signal reflects the conductance change $\delta G(x,y,z)$ as the tip is scanned over lateral coordinates x and y at height z above the surface. The potential on the tip will change the conductance by locally modulating the charge density. It may also modify the scattering, though the former is likely to be the dominant effect, and in any case the distinction between the two effects is not clear-cut. Whatever the mechanism, we assume for simplicity that δG is proportional to the change in charge density at the sensitive point, that the charge density is linear in V_{tip}, and that $\delta G = 0$ when the tip is grounded. Then $\delta G \propto C_{ts}(x,y,z)V_{tip}$, where $C_{ts}(x,y,z)$ is the capacitance to the tip per unit area of the sample at the sensitive point.[18] The slow (reciprocal) fall off of capacitance with distance is responsible for the low resolution and nonlocality of SGM. For $z \gtrsim 5$ nm, the capacitances to the tip cone and cantilever exceed that to the tip apex.[19] As a result the response to the sensitive point includes a large "nonlocal" part spread over a lateral area comparable with the size of the tip cone (of order 10 μm) and the cantilever (of order 30 μm by 150 μm). Many samples, such as 2D films, are sensitive at multiple points or over extended areas, and the combination of the nonlocal response from all sensitive regions produces a large and obfuscating background which in most cases cannot be deconvolved.

In tmSGM the situation is different. When the tip oscillates mechanically at its resonant frequency ω with a small amplitude z_ω, it causes C_{ts} to oscillate by an amount $C_\omega = (\partial C_{ts}/\partial z)z_\omega$. This in turn causes an oscillation of the conductance of amplitude $G_\omega \propto C_\omega(x,y,z)V_{tip}$ which is measured by the lock-in amplifier. The resulting signal is therefore proportional to $\partial C_{ts}/\partial z$. The relative contributions of cantilever and tip cone to $\partial C_{ts}/\partial z$ are much smaller than their contributions to C_{ts}, roughly speaking because the spatial derivative of the capacitance decays as the inverse square of distance rather than just the reciprocal.

This situation resembles that in force-sensitive EFM, where the force on the tip, determined by the gradient of the electrostatic energy, is proportional to the first derivative of the total tip−sample capacitance. The EFM

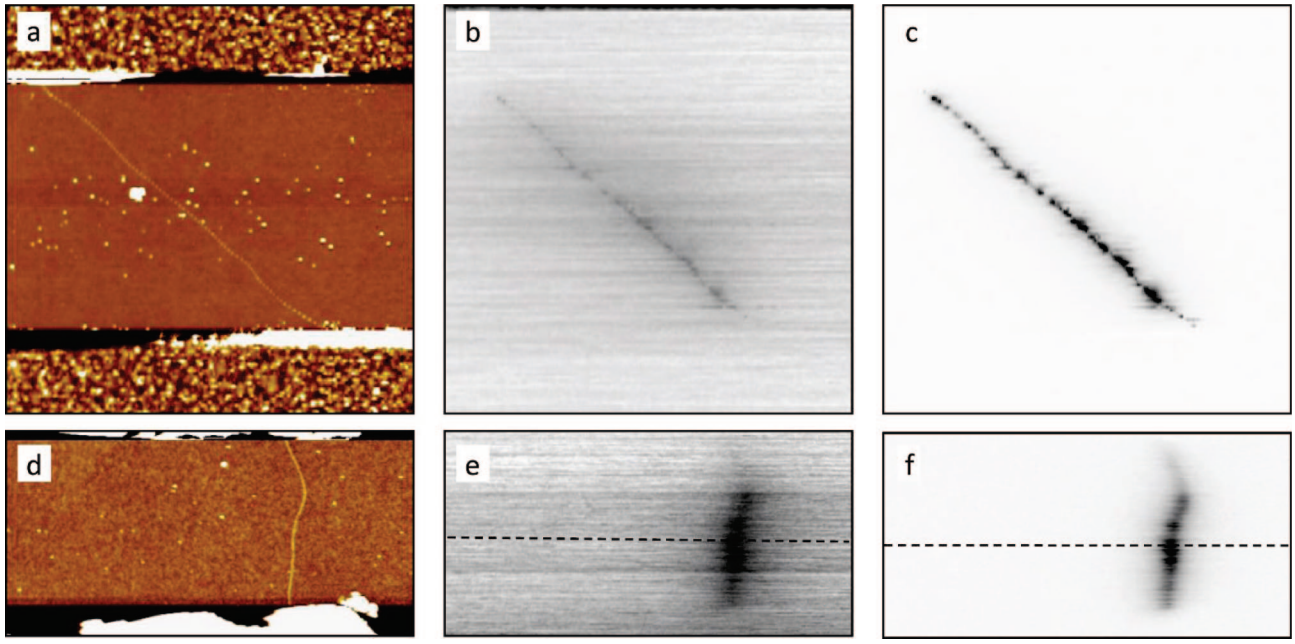

Figure 2. Images of two nanotube devices. Upper panels, device 1: (a) topography (20 nm full scale), (b) SGM, and (c) tmSGM. The scan is 5 μm square, and $V_{tip} = 2.5$ V, $V_{sd} = 0.1$ V, $V_g = 0$ V, and $l_h = 20$ nm. Lower panels, device 2: (a) topography (10 nm full scale), (b) SGM and (c) tmSGM. The scan is 4 microns wide, and $V_{tip} = 10$ V, $V_{sd} = 0.5$ V, $V_g = 0$ V, and $l_h = 20$ nm. The dashed lines correspond to the line profiles shown in Figure 3.

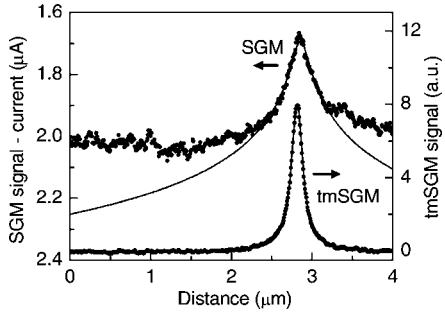

Figure 3. Line profiles from the SGM (left axis) and tmSGM (right axis) images in Figure 2. The solid lines are fits as described in the text.

signal from a nanotube on an insulator is known to be well described empirically by a Lorentzian function of the distance x perpendicular to the nanotube.[16,17] We find that tmSGM peaks such as the one in Figure 3 are also accurately fit by Lorentzians, consistent with the parallel between tmSGM and EFM. The narrower line width for tmSGM compared with SGM can then be quantified as follows. A Lorentzian tmSGM profile implies that $\partial C_{ts}(x,y,z)/\partial z \approx a/(4x^2 + w^2)$, where the height a and width w are independent of x. Assuming that both a and w are approximately proportional to z, as is the case for EFM,[17] we can integrate to find that the peak in $C_{ts}(x,y,z)$, and hence the corresponding SGM signal, should have the form $b\ln(4x^2 + w^2)$, where b is independent of x. This logarithmic peak decays more slowly than the Lorentzian, and has broad shoulders with no asymptotic background level. Indeed, the bulk of the feature in the SGM signal in Figure 3 is accurately described by this logarithmic function, where b is the only fitting parameter because $w = 175$ nm has been determined from the Lorentzian fit to the tmSGM signal. At distances $\gtrsim 1$ μm away from the center of the peak, the SGM signal deviates from the logarithmic function, although it does not become flat. This is not surprising because of the undesirable long-range contributions from the tip cone and cantilever which are expected to be present on such a scale.

Having shown that tmSGM is related to the gradient of the capacitance we can also comment on the spatial resolution. The lateral resolution of EFM has been the subject of much study and has been found to be dependent on factors such as tip radius of curvature,[20] oscillation amplitude, lift height,[17] and tip geometry (with a long thin probe being optimal[20]). We expect the same to be true for tmSGM.

As mentioned in the introduction, the advantages of tmSGM are such that it can be more useful than SGM for studying two-dimensional samples. We illustrate this using 2D nanotube network devices, which have potential uses as sensors[21] and in plastic and transparent electronics.[22,23] Figure 4a is a topographic image of a random 2D network of nanotubes on an SiO_2 substrate. The nanotubes outside the region between the two metal contact electrodes at the top and bottom were removed by a final etching step (O_2 RF plasma etch, 100 W for 1 min at 0.6 mbar).[24] The larger lumps visible here are photoresist residue. It would be useful to understand what determines the conductivity of such a network, in which there are a large number of current paths. For example, in chemical sensing applications, identifying whether it is the junctions or certain nanotubes that dominate the transconductance will help in tailoring the binding interactions of functional molecules to the nanotubes to give optimal performance.

Figure 4b is an EFM measurement of the same device, made by applying an ac voltage of 1 V rms at the cantilever

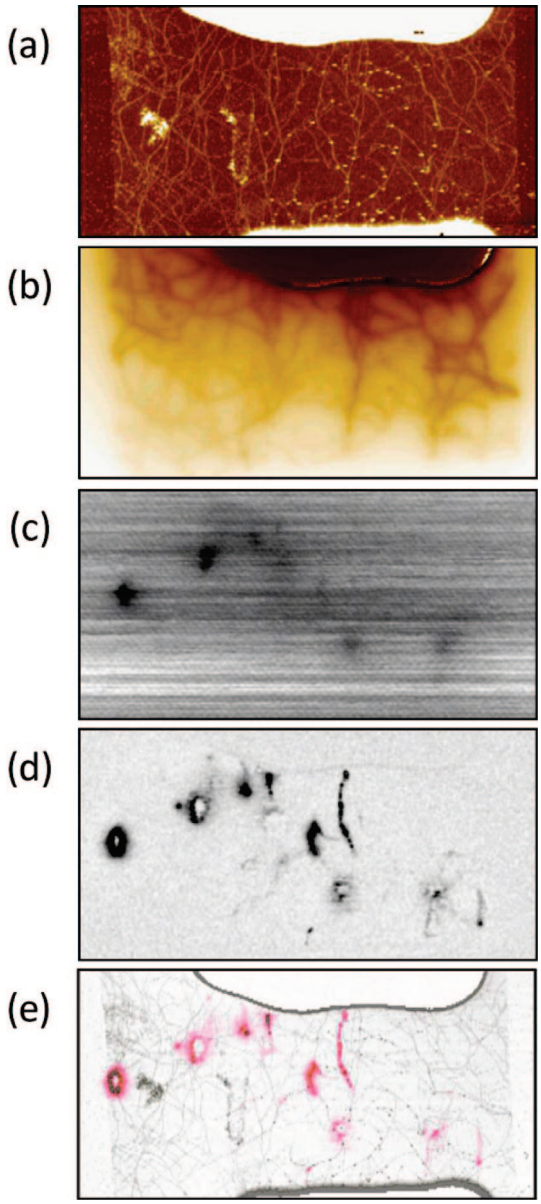

Figure 4. Images of a nanotube network device: (a) topography (30 nm full scale), (b) EFM, (c) SGM, (d) tmSGM, and (e) superposition of tmSGM on height image. The scans are 14 μm wide. In the EFM measurement $V_{sd} = 1$ V_{rms}, $V_{tip} = 12$ V, and $l_h = 40$ nm; in the (tm)SGM measurements, $V_{sd} = 0.1$ V, $V_{tip} = 12$ V, and $l_h = 20$ nm. The data in panels a and b were taken simultaneously, as were those in panels d and e, but there is a slight positional shift between the former and the latter.

resonant frequency to the source contact with no voltage on the cantilever drive piezo, and with $V_{tip} = +12$ V dc. In this configuration, the cantilever oscillation amplitude roughly reflects the local ac potential on the surface. The potential distribution is visibly inhomogeneous over the network, but extracting information from such a measurement on its own is difficult: parallel paths with very different resistances can present similar patterns of voltage drop, and the signal when the tip is over the insulating substrate cannot be easily interpreted.

Scanned gate techniques could provide important complementary information to such EFM measurements. Figure 4c is a conventional SGM image of the same device. Several dark patches can be distinguished, showing that some parts of the network have high sensitivity to the tip bias. However, these patches are too blurred to be associated with specific network features. Figure 4d is a tmSGM image of the same device recorded under the same conditions. Numerous features can be resolved that are indistinguishable from background noise in the SGM image and that are sharp enough to be linked to specific nanotubes or intratube junctions, as illustrated by the superposition of height and tmSGM images in Figure 4e. TmSGM is thus able to identify the features in the network that dominate the transconductance. We see that the sensitivity tends to be large at isolated points rather than along the length of nanotube segments, indicating the conductivity is determined mainly by defects and intratube junctions.

In summary, we have introduced a new technique, called tmSGM, which increases the spatial resolution and sensitivity of scanned gate microscopy by measuring the conductance change in response to the oscillation of a biased tip. Most importantly, unlike conventional SGM, tmSGM yields a local measurement that enables accurate mapping of samples in which multiple parallel conducting paths exist. We developed and assessed the technique by applying it to nanotube networks. It should be useful in studying a variety of other 2D materials such as thin conducting polymer films and graphene.

Acknowledgment. This work was supported in part by the EPSRC (EP/C518268/1) and in part by the Army Research Office under contract number 48385-PH.

References

(1) Kuntze, S.; Ban, D.; Sargent, E.; Dixon-Warren, S.; White, J.; Hinzer, K. *Crit. Rev. Solid State* **2005**, *30* (2), 71–124.
(2) Tans, S. J.; Dekker, C. *Nature* **2000**, *404* (6780), 834.
(3) Park, J.-Y.; Yaish, Y.; Brink, M.; Rosenblatt, S.; McEuen, P. L. *Appl. Phys. Lett.* **2002**, *80* (23), 4446–4448.
(4) Bachtold, A.; Fuhrer, M. S.; Plyasunov, S.; Forero, M.; Anderson, E. H.; Zettl, A.; McEuen, P. L. *Phys. Rev. Lett.* **2000**, *84* (26), 6082–6085.
(5) Freitag, M.; Johnson, A. T.; Kalinin, S. V.; Bonnell, D. A. *Phys. Rev. Lett.* **2002**, *89* (21), 4.
(6) Freitag, M.; Radosavljevic, M.; Zhou, Y.; Johnson, A. T.; Smith, W. F. *Appl. Phys. Lett.* **2001**, *79* (20), 3326.
(7) Bockrath, M.; Liang, W. J.; Bozovic, D.; Hafner, J. H.; Lieber, C. M.; Tinkham, M.; Park, H. K. *Science* **2001**, *291* (5502), 283–285.
(8) Woodside, M. T.; McEuen, P. L. *Science* **2002**, *296* (5570), 1098–1101.
(9) Zhou, X.; Dayeh, S. A.; Wang, D.; Yu, E. T. *Appl. Phys. Lett.* **2007**, *90* (23), 3.
(10) Eriksson, M. A.; Beck, R. G.; Topinka, M.; Katine, J. A.; Westervelt, R. M.; Campman, K. L.; Gossard, A. C. *Appl. Phys. Lett.* **1996**, *69* (5), 671–673.
(11) Aoki, N.; da Cunha, C. R.; Akis, R.; Ferry, D. K.; Ochiai, Y. *Phys. Rev. B* **2005**, *72* (15), 4.
(12) Topinka, M. A.; LeRoy, B. J.; Westervelt, R. M.; Shaw, S. E. J.; Fleischmann, R.; Heller, E. J.; Maranowski, K. D.; Gossard, A. C. *Nature* **2001**, *410* (6825), 183–186.
(13) Crook, R.; Smith, C. G.; Tribe, W. R.; O'Shea, S. J.; Simmons, M. Y.; Ritchie, D. A. *Phys. Rev. B* **2002**, *66* (12), 121301.
(14) Nonnenmacher, M.; Oboyle, M. P.; Wickramasinghe, H. K. *Appl. Phys. Lett.* **1991**, *58* (25), 2921–2923.
(15) Gil, A.; Colchero, J.; Gomez-Herrero, J.; Baro, A. M. *Nanotechnology* **2003**, *14* (2), 332–340.
(16) Kalinin, S. V.; Bonnell, D. A.; Freitag, M.; Johnson, A. T. *Appl. Phys. Lett.* **2002**, *81* (4), 754.
(17) Wilson, N. R.; Macpherson, J. V. *J. Appl. Phys.* **2004**, *96* (6), 3565–3567.

(18) For small separations the tip-sample capacitance can be approximated by that of a sphere above a conducting surface, which gives about 10^{-17} F. Previous investigations have estimated tip-nanotube capacitances to be of order 10^{-18} F (see, e.g., Bockrath et al. *Nano Lett.* **2002**, *2*, (3), 187−190).
(19) Colchero, J.; Gil, A.; Baro, A. M. *Phys. Rev. B* **2001**, *64* (24), 245403.
(20) Jacobs, H. O.; Leuchtmann, P.; Homan, O. J.; Stemmer, A. *J. Appl. Phys.* **1998**, *84* (3), 1168–1173.
(21) Gruner, G. *Anal. Bioanal. Chem.* **2006**, *384* (2), 322–35.
(22) Gruner, G. *J. Mater. Chem.* **2006**, *16* (35), 3533–3539.
(23) Snow, E. S.; Novak, J. P.; Lay, M. D.; Houser, E. H.; Perkins, F. K.; Campbell, P. M. *J. Vac. Sci. Technol. B* **2004**, *22* (4), 1990–1994.
(24) Edgeworth, J. P.; Wilson, N. R.; Macpherson, J. V. *Small* **2007**, *3* (5), 860–870.

NL080488I